International Journal of Heat and Mass Transfer 119 (2018) 867–879

Contents lists available at ScienceDirect

International Journal of Heat and Mass Transfer

journal homepage: www.elsevier.com/locate/ijhmt

A validated time-stepping analytical model for 3D transient vapor chamber transport

Gaurav Patankar, Justin A. Weibel, Suresh V. Garimella *

Cooling Technologies Research Center, School of Mechanical Engineering, Purdue University, 585 Purdue Mall, West Lafayette, IN 47907, USA

ARTICLE INFO

Article history:
Received 24 May 2017
Received in revised form 22 November 2017
Accepted 27 November 2017

Keywords:
Vapor chamber
Heat pipe
Heat spreaders
Transient
Low-cost modeling

ABSTRACT

Advances in the computational performance of electronic devices have created a clear need for improved methods of passive thermal management. This has led to renewed interest in the use of vapor chambers as heat spreaders in applications ranging from mobile devices to high-performance-computing and power electronics systems. While there has been significant effort to develop vapor chambers for these applications, their designs have largely relied on steady-state analyses and performance prediction. In many applications, however, the heat load is inherently transient in nature. Heat spreader design must consider transient performance in response to these use-case scenarios. While detailed numerical models of transient vapor chamber operation have been developed, a transient modeling approach with low computational cost is needed for parametric study and quick assessment of vapor chamber performance in system-level models.

In the current work, a low-cost, transient vapor chamber model is developed targeting the geometries and operating conditions typical of thermal management applications. The model considers mass, momentum, and energy transport in the vapor chamber wall, wick, and vapor core as well as phase change at the wick-vapor interface. The governing equations are simplified to a system of first-order differential equations based on a scaling analysis and assuming a functional form for the temperature profile along the thickness dimension. The errors in the temperature and pressure fields due to these simplifying assumptions are estimated for a wide range of operating conditions. These estimates indicate low errors in the model predictions over the range considered. For two example cases, the model predictions are compared to a finite-volume-based numerical model. Any deviation from the numerical model prediction is on the same order as the errors estimated based on the simplifying assumptions. The time-stepping analytical model is demonstrated to have a computational cost reduction of three to four orders of magnitude compared to the finite-volume based model.

1. Introduction

A vapor chamber passively spreads heat from a small heat source to a larger surface. The sealed chamber is typically lined on the inner surface with a porous wick material and has a hollow central core; the device is charged with a working fluid that is held in the wick as liquid and vaporizes into the core. Operation of the vapor chamber is illustrated in Fig. 1. Heat input to the vapor chamber causes localized vapor generation at the wick–vapor interface, which spreads through the core. As vapor condenses at the colder wick–vapor interface, the heat released is conducted across the condenser-side wick and the wall to the heat rejection surface. Condensed liquid is pumped back to the evaporator in the porous wick via capillary forces, enabling continuous passive operation.

Vapor chambers and heat pipes are used in the thermal packaging of electronic components as integrated heat spreaders for a variety of applications. The heat flux dissipated ranges from <10 W/cm^2 for applications such as portable electronics [1] to >500 W/cm^2 for cooling of radar power amplifiers and high-performance computing systems [2]. Common among these applications is the need for thin, compact heat spreaders that accommodate transient heat loads. For example, mobile electronic devices require heat spreaders of <1 mm thickness and experience highly transient operation; idle periods of low heat generation are intermixed with shorter pulses of high-power operations (*e.g.*, video recording or calling). Previous work in designing vapor chambers for mobile devices has been limited to a consideration of steady-state operation [3]. Evaluation of vapor chambers for

* Corresponding author.
E-mail address: sureshg@purdue.edu (S.V. Garimella).

https://doi.org/10.1016/j.ijheatmasstransfer.2017.11.135
0017-9310/

Nomenclature

$\underset{\sim}{A}$, $\underset{\sim}{B}$	matrix containing thermophysical and geometric properties
$\underline{b}_{lk}$	coefficients of 2D Fourier series [K s^{-1}]
$\underline{C}$	vector source term [K s^{-1}]
$\underline{a}_{lk}$, c_{lk}	coefficients of 2D Fourier series [K]
CN_{CC}	condition number for linearizing the Clausius-Clapeyron equation
CN_{conv}	condition number for assuming negligible convection in the momentum equation in the vapor core
CN_T	condition number for assuming negligible temperature difference across the thicknesses of the wall and the wick on the evaporator side
$d_{sum,lk}$, $d_{diff,lk}$	coefficients of 2D Fourier series [Pa]
d_p	wick particle diameter [m]
ρC_p	volumetric specific heat capacity [J kg^{-1} K^{-1}]
h	convection coefficient [W m^{-2} K^{-1}]
h_{fg}	specific enthalpy of vaporization [J kg^{-1}]
h_{vap}	thickness of vapor core [m]
$h_{wall,\,1}$	thickness of evaporator-side wall [m]
$h_{wall,\,2}$	thickness of condenser-side wall [m]
$h_{wick,\,1}$	thickness of evaporator-side wick 1 [m]
$h_{wick,\,2}$	thickness of condenser-side wick 2 [m]
K	permeability of the porous medium [m^2]
k	thermal conductivity [W m^{-1} K^{-1}]
k_{eff}	porous medium effective thermal conductivity [W m^{-1} K^{-1}]
L_x	length of the vapor chamber in x direction [m]
L_y	width of the vapor chamber in y direction [m]
l, k	indices of summations in the 2D Fourier series [–]
$\dot{m}''$	mass flux rate due to phase change [kg m^{-2} s^{-1}]
N	number of terms in truncated infinite series
P	pressure [Pa]
P_{cap}	capillary pressure [Pa]
P_O	saturation pressure corresponding to the volume-averaged vapor core temperature [Pa]
Pr	Prandtl number $\left(\frac{\mu}{\rho\alpha}\right)$ [–]
q''_{in}	external boundary heat flux [W m^{-2}]
R	specific gas constant [J kg^{-1} K^{-1}]
Re	Reynolds number $\left(\frac{\rho UL}{\mu}\right)$ [–]
T	temperature [K]
$\bar{T}$	z-averaged temperature [K]
T_{sat}	saturation temperature [K]
T_∞	ambient temperature [K]
t	time [s]
$\underset{\rightarrow}{u}$	x-component of velocity [m s^{-1}]
V	velocity vector [m s^{-1}]
v	y-component of velocity [m s^{-1}]
w	z-component of velocity [m s^{-1}]
x	x-coordinate (length) direction [m]
y	y-coordinate (width) direction [m]
z	z-coordinate (thickness) direction [m]

Greek

α	thermal diffusivity $(k_{eff}/(\rho C_p)_{eff})$ [m^2 s^{-1}]
γ	surface tension [Pa s]
ε_{CC}	relative error in the pressure field due to linearization of the Clausius-Clapeyron equation
ε_{conv}	relative error in the pressure field due to neglecting convection in the momentum equation in the vapor core
ε_T	relative error in the temperature field due to neglecting temperature difference across the thicknesses of the wall and the wick on the evaporator side
$\underline{\Theta}$	vector of temperature field variables [K]
λ	constant $\left(\frac{h_{fg}P_O}{R(T_{sat}^2)_{mean}}\right)$ [Pa K^{-1}]
μ	viscosity [Pa s]
ρ	density [kg m^{-3}]
σ	accommodation coefficient [–]
φ	constant $\left(\frac{2\sigma}{2-\sigma}\frac{h_{fg}\rho_{vap}}{(T_{vap}^{1.5})_{mean}}\left(\frac{1}{2\pi R}\right)^{0.5}\right)$ [kg m^{-2} s^{-1} K^{-1}]
ϕ	porosity [–]

Subscript

int	wick–vapor interface
sum	wick 1 plus wick 2
diff	wick 1 minus wick 2
vap	corresponding to the vapor core
wall	corresponding to the wall
wick	corresponding to the wick
x	along x coordinate direction
y	along y coordinate direction
z	along z coordinate direction
1	corresponding to the evaporator side
2	corresponding to the condenser side

Superscript

n	time step
0	initial condition

Vector notation

–	Vector
~	Matrix

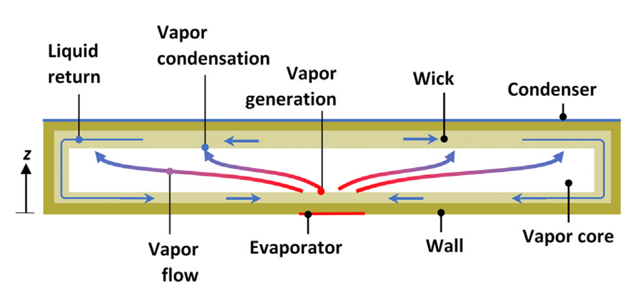

Fig. 1. Cross-sectional view of vapor chamber operation that illustrates the key components and transport mechanisms.

mobile devices and other applications will require transport models capable of efficiently computing the temperature field for transient boundary conditions and thin form factors.

Existing vapor chamber transport models introduce a range of complexities that typically represent a compromise between computational cost and fidelity. Discretized numerical models are capable of simulating the transient behavior of complex vapor chamber geometries under different operating conditions. Such models are only limited by assumptions inherent in the governing equations used to represent the transport mechanisms. Vadakkan et al. [4] and Ranjan et al. [5,6] developed a finite-volume-based numerical model to solve the mass, momentum, and energy transport equations in the wall, wick, and vapor core of the vapor cham-